BIOCHEMISTRY
including biophysical chemistry & molecular biology
Article

Biochemistry **2011,** *50,* 1839–1847 1839
DOI: 10.1021/bi102076s

Binding Properties of the Calcium-Activated F2 Isoform of *Lethocerus* Troponin C†

Stephen R. Martin,[‡,#] Giovanna Avella,[‡,§,#] Miquel Adrover,[∥] Gian Felice de Nicola,[⊥] Belinda Bullard,[@] and Annalisa Pastore*[,‡]

[‡]*National Institute for Medical Research, The Ridgeway, London NW71AA, U.K.,* [§]*Dip. di Scienze Biochimiche "A. Rossi Fanelli", Universita' degli Studi di Roma "La Sapienza", 00185 Roma, Italy,* [∥]*Departament de Química, IUNICS, Universitat de les Illes Balears, Palma de Mallorca, Spain,* [⊥]*King's College, The Randall Division, New Hunt's House, Guy's Campus, London SE11UL, U.K., and* [@]*Department of Biology, University of York, York YO10 5DD, U.K.* [#]*These authors contributed equally to this work.*

Received December 31, 2010; Revised Manuscript Received January 19, 2011

ABSTRACT: While in most muscles contraction is triggered by calcium effluxes, insect flight muscles are also activated by mechanical stretch. We are interested in understanding the role that the troponin C protein, usually the calcium sensor, plays in stretch activation. In the flight muscles of *Lethocerus*, a giant water bug often used as a model system, there are two isoforms of TnC, F1 and F2, present in an approximately 10:1 ratio. F1 TnC is responsible for activating the muscle following a stretch, whereas F2 TnC produces a sustained contraction, the magnitude of which depends on the concentration of Ca^{2+} in the fiber. We have previously shown that F1 TnC binds only one Ca^{2+} ion in its C-terminal domain and that interaction with troponin H, the insect ortholog of troponin I, is insensitive to Ca^{2+}. Here, we have studied the effect of Ca^{2+} and Mg^{2+} on the affinities of the interaction of F2 TnC with troponin H peptides. We show that the presence of two Ca^{2+} ions, one in each of the globular domains, increases the affinity for TnH by at least 1 order of magnitude. The N lobe has a lower affinity for Ca^{2+}, but it is also sensitive to Mg^{2+}. The C lobe is insensitive to Mg^{2+} as previously demonstrated by mutations of the individual EF-hands. The interaction with TnH seems also to have significant structural differences from that observed for the F1 TnC isoform. We discuss how our findings could account for stretch activation.

Muscle contraction is initiated by impulses from the motor neurons to the muscle that cause depolarization of the innervated fibers (see refs (*1*−*3*) for reviews). In synchronous muscles, an action potential triggers release of Ca^{2+} from an internal store within the fiber, the sarcoplasmatic reticulum. The released Ca^{2+} diffuses into the myofibrils, binds to control sites on the contractile filaments, and initiates contraction. This contraction is terminated when the sarcoplasmatic reticulum resequesters the released Ca^{2+} and reduces its cytoplasmatic concentration to a level below the threshold required for contractile activity.

The Ca^{2+} sensor that regulates this process resides in the tropomyosin−troponin complex. In the absence of Ca^{2+}, tropomyosin, a rodlike protein that extends over seven actin monomers, blocks the myosin-binding sites present on the thin filament (*3*−*5*). Troponin is a complex of three regulatory proteins: a Ca^{2+} binding protein (TnC), an inhibitory protein (TnI), and a tropomyosin binding protein (TnT) (*6*). TnC senses Ca^{2+} through up to four Ca^{2+} binding motifs (EF-hands) distributed across two globular domains, the N- and C-terminal domains (*7*−*11*). The C-terminal domain (C lobe) usually interacts with an N-terminal region of TnI and anchors it into a specific conformation (*12*−*15*). When the N-terminal domain (N lobe) of TnC is able to bind Ca^{2+}, it undergoes a conformational transition that allows it to bind to the "switch peptide" of TnI (residues 115−131 of skeletal TnI) (*12*), initiating the tropomyosin movement that causes the generation of force.

In some muscles, however, such as in the flight muscles of many insects, contraction is not simply regulated by the Ca^{2+} switch. The wing beat frequency is too high for individual contractions of the flight muscles to be activated by Ca^{2+} (*16*−*19*). To adapt to this requirement, indirect flight muscles (IFM) have evolved two distinct forms of activation, which are finely tuned to the type of movement required (*20*, *21*): a stretch-activated mechanism (asynchronous contraction) is used for flying, whereas Ca^{2+} regulation remains important during the "warm-up" contractions that precede flight in large insects (synchronous contraction). During flight, stretch and Ca^{2+} activation are finely balanced, depending on the Ca^{2+} concentration produced by the intermittent nerve impulses (*20*−*22*).

Despite its importance for understanding the mechanisms of muscle contraction, relatively little is known about stretch activation and the way it coexists with synchronous regulation, although current evidence all seems to indicate that the muscle regulation in insects differs markedly from that of vertebrates. Most of our knowledge about insect muscles comes from studies of *Lethocerus*, a giant water bug of the Belostomatidae family, native to Southeast Asia, which is commonly used as a model system because its large muscle fibers are easily manageable. In *Lethocerus*, two isoforms of TnC coexist in the same myofibril, F1 and F2, in a ratio of ∼10:1 (*23*, *24*). F1 TnC, which has a single Ca^{2+} binding site in the C lobe, is responsible for activating the muscle following a stretch. F2 TnC has two Ca^{2+} binding sites, one in each lobe, and produces a sustained contraction, the magnitude of which is dependent on the Ca^{2+}

†This research was funded by the Medical Research Council (Grant U117584256) and the EU sixth framework network of excellence MYORES.

*To whom correspondence should be addressed. Telephone: 0044-20-88162630. Fax: 0044-20-89054477. E-mail: apastor@nimr.mrc.ac.uk.

Published on Web 01/20/2011

concentration (*20*). In previous studies, we have shown that the C lobe of F1 TnC binds to peptides spanning the N-terminal and inhibitory regions of TnH [the insect equivalent of TnI (*25*)], although with very different affinities (*26*). The equilibrium dissociation constant for the complex with the N-terminal TnH peptide is in the nanomolar range, which is comparable to the values reported for the skeletal TnC−TnI complex (*27*, *28*). The affinity for the peptide from the inhibitory region is much lower, in the micromolar range, which is comparable to the affinity of the inhibitory peptide of skeletal TnI for the C lobe of TnC (*29*). Both interactions are essentially Ca^{2+} independent, and the N lobe of F1 TnC appears to play no role. It was therefore suggested that competition between two distinct regions of TnH, which alternately occupy the C lobe of F1 TnC, could be the basis of stretch activation. The relative affinity of F1 TnC and F2 TnC for the whole TnI sequence in TnH, in the presence of Ca^{2+}, has been determined (*24*). The overall affinity of F2 TnC is greater than that of F1 TnC, which is likely caused by the two binding sites for TnI in F2 TnC and the single site in F1 TnC.

Here, we have used a range of biophysical techniques to dissect the interaction of F2 TnC into specific contributions using synthetic peptides from TnH and studied how the complex affinities are modulated by the presence of Ca^{2+} and/or Mg^{2+}. We show that F2 TnC binds to the same regions of TnH as F1 TnC but with two important differences. First, the interaction of F2 TnC with the peptides shows significant Ca^{2+} dependence, and second, interaction with the peptides does not involve just the TnC C lobe but causes a more generalized conformational change. Our data improve our understanding of Ca^{2+} regulation of insect flight muscle.

EXPERIMENTAL PROCEDURES

Protein Production. *Lethocerus* F2 TnC cDNA was inserted into the *Nco*I and *Not*I sites of a modified pET24d (M11) expression vector (Novagen) containing an N-terminal hexahistidine tag followed by a tobacco etch virus (TEV) protease cleavage site. The construct was further subcloned to produce individually the two lobes (residues 1−88 and 89−158) of F2 TnC into the pETDTDuet-1 vector using *Bam*HI and *Pst*I sites. The following forward and reverse primers were used: 5′-atggatccagaaaacctgtacttccaaggaatggtcgccatggatgatctggac-3′ (forward primer) and 5′-cggtcatgctgcagttatcaggcggccgaatcttcttcgttgtcttc-3′ (reverse primer) for the N-terminal lobe and 5′-atggatccagaaaacctgtacttccaaggaatgatggaagagctcagggaggc-3′ (forward primer) 5′-cggtcatgctgcagttatcactcgtccccaccgatcatcacttc-3′ (reverse primer) for the C-terminal lobe.

The constructs were transformed through a heat shock protocol using BL21(DE3) or BL21(DE3) pLysS competent cells (Stratagene). The plasmid DNA (1 μL at concentrations of 50−100 ng/μL) was added to 50 μL of competent cells kept on ice for 30 min and then heat shocked at 42 °C for 45−50 s followed by incubation on ice for 2 min. Luria-Bertani (LB) broth (1 mL) was added to the cells, which were left at 37 °C for 30 min and then allowed to grow on LB agar plates containing kanamycin (0.1 mg/mL) at 25 °C for 24 h. The growth was used to inoculate 1 L of medium, and the cells were grown at 25 °C. When the OD_{600} reached 0.7−0.8, isopropyl β-D-thiogalactopyranoside (IPTG) was added at a final concentration of 0.2 mM to induce protein production. Isotopically labeled samples were produced by growing the cells in minimum medium supplemented with $[^{13}C_6]$glucose and $^{15}NH_4Cl$ as the sole carbon and nitrogen sources, respectively.

A similar purification strategy was used for all constructs. Cells were centrifuged at 4 °C, and the pellet was resuspended in lysis buffer containing 150 mM NaCl, 10 mM imidazole, 20 mM Tris-HCl (pH 8), lysozyme, DNase I, $MgCl_2$, the COMPLETE EDTA free protease inhibitor cocktail (Roche), and PMSF. The lysate was sonicated on ice, and the supernatant was collected after centrifugation at 20000 rpm for 40 min at 4 °C. The His_6-tagged protein was purified with a Ni^{2+}-nitrilotriacetate (Ni-NTA)−agarose column (Qiagen) and eluted with 100 mM imidazole in the same buffer. All fractions were checked on a 12% acrylamide gel. The His_6 tag was removed using TEV protease (*30*) incubation at 4 °C for 16 h. The cleaved His_6 tag and the residual TEV were removed when the sample was loaded onto Ni^{2+}-nitrilotriacetate (Ni-NTA)−agarose columns (Qiagen) equilibrated in 20 mM Tris-HCl (pH 8) and 150 mM NaCl. The proteins were further purified by size exclusion chromatography using a Superdex 75 26/60 column (Pharmacia) equilibrated with a buffer containing 100 mM NaCl and 20 mM Tris-HCl (pH 6.8).

Ca^{2+}-free (apo) F2 TnC was prepared by mixing concentrated samples of the protein with 5 mM EGTA. These samples were then desalted by two passes through Pharmacia G-25 PD10 columns equilibrated with Ca^{2+}-free (Chelex-100-treated) buffer [20 mM Tris-HCl (pH 6.8) and 100 mM NaCl]. The residual Ca^{2+} concentration in the buffer was estimated to be < 1 μM using the chromophoric Ca^{2+} chelator 5,5′-Br_2BAPTA.

Peptides. Peptides TnH(30−61) (YKAKKAKKGFMTPERKKKLRLLLRKKAAEELKK) and TnH(126−159) (YDLNSQVNDLRGKFVKPTLKKVSKYENKFAKLQKK) were purchased from Peptide 2.0 Inc. Melittin from honey bee venom was purchased from Sigma-Aldrich Co. (Dorset, U.K.). The purity of the peptides was greater than 95% as assessed by HPLC, and the sequences were verified using MALDI mass spectroscopy.

Fluorescence Measurements. Uncorrected fluorescence emission spectra were recorded using a Jasco FP-6300 spectrofluorimeter equipped with an ETC-273T temperature controller with excitation at 280 nm (bandwidth of 1.5 nm) and emission scanned from 290 to 400 nm (bandwidth of 5 nm). All measurements were taken at 20 °C in 20 mM Tris-HCl (pH 6.8) and 100 mM NaCl.

CD Measurements. Near- and far-UV CD spectra were recorded on a Jasco J-715 spectropolarimeter equipped with a PTC-348WI temperature controller. Near-UV CD intensities are presented as the CD absorption coefficient calculated using the molar concentration of protein ($\Delta\varepsilon_M$) and far-UV CD intensities as the CD absorption coefficient calculated on a mean residue weight basis ($\Delta\varepsilon_{MRW}$). Thermal denaturation was followed by monitoring the far-UV CD signal at 222 nm while changing the temperature from 2 to 95 °C at a rate of 1 °C/min. All CD measurements were taken in 10 mM Hepes (pH 6.8) and 100 mM NaCl.

Ca^{2+} Binding Studies. Stoichiometric Ca^{2+} association constants for F2 TnC in the presence and absence of the TnH peptides were determined from Ca^{2+} titrations of apoprotein samples performed in the presence of the chromophoric Ca^{2+} indicators, 5,5′-dibromo BAPTA and 5-nitro BAPTA, using published methods (*31*). Measurements were performed at 20 °C in 20 mM Tris-HCl (pH 6.8) and 100 mM NaCl using a JASCO V-550 UV−vis spectrophotometer equipped with an ETC-505T temperature controller. The equilibrium association constants for 5,5′-dibromo BAPTA and 5-nitro BAPTA under these conditions were determined to be $(6.3 \pm 0.5) \times 10^5$ and $(4.1 \pm 0.3) \times 10^4$ M^{-1}, respectively.

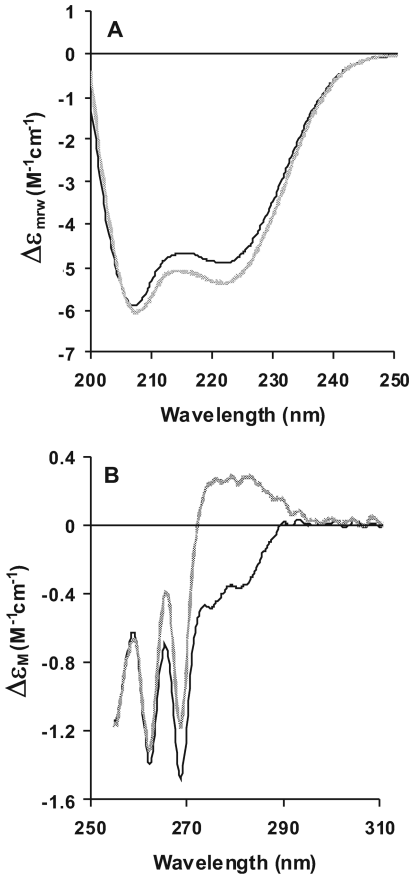

FIGURE 1: Probing the secondary structure of F2 TnC by CD spectroscopy. CD spectra of F2 TnC in the absence (black lines) and presence (gray lines) of 1 mM Ca^{2+}. We estimated ~50% helical content using the methods described in ref *41*. (A) Far-UV spectra. (B) Near-UV spectra.

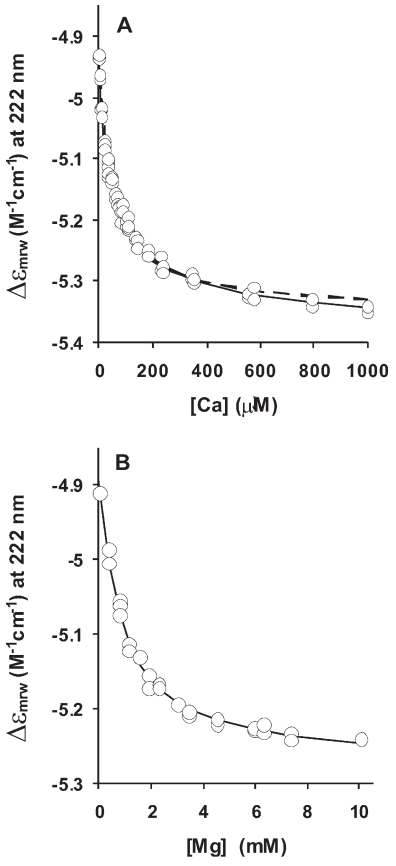

FIGURE 2: Effects of Ca^{2+} and Mg^{2+} on F2 TnC. Far-UV CD titrations of apo F2 TnC with Ca^{2+} (A) and Mg^{2+} (B). The solid lines are fits to two-site (A) and one-site (B) binding models. The dashed line in panel A is the best fit to a one-site model (χ^2 of 4.8 compared with 1.2 for the fit to the two-site model).

NMR Measurements. All NMR experiments were carried out at 25 °C and 600 MHz on a Varian Inova or an Advanced Bruker spectrometer equipped with a cryoprobe. The concentrations of highly concentrated stock solutions of the peptides, in 100 mM KCl and 20 mM Tris-HCl, were measured in triplicate by amino acid analysis. The pH was adjusted to 6.8 with small additions of a 0.01 M NaOH solution. The pH was checked after the final peptide addition to make sure that it had remained constant throughout the titration. The final F2 TnC:TnH(30−61) and TnC:TnH(126−159) molar ratios were 1:3 and 1:2.5, respectively. At these molar ratios, two successive additions of peptides did not produce further changes in the spectra.

RESULTS

CD Studies of F2 TnC. The far-UV CD spectra of the apo and Ca^{2+}-loaded forms of F2 TnC (Figure 1A) are those of a protein with a high α-helical content (~50%), indicating that the protein is folded also in the absence of the cation. The Mg^{2+}-induced change in CD intensity is similar to, though slightly smaller than, that induced by Ca^{2+} (not shown), indicating that both metal ions perturb the secondary structure (as reflected by CD) in a similar way. The near-UV CD spectra of the apo and Ca^{2+}-loaded forms of F2 TnC (Figure 1B) show that Ca^{2+} also causes a change in the tertiary structure of the protein close to one or more of the three tyrosine residues. The near-UV CD spectrum of the Mg^{2+}-loaded form is essentially identical to that of the apoprotein, showing that Mg^{2+} binding does not perturb the environment of the tyrosine residues.

Although the change in the far-UV CD signal is small, it can be used to monitor binding of a metal ion to F2 TnC. The far-UV CD titration of apo F2 TnC with Ca^{2+} (Figure 2A) could not be satisfactorily analyzed with a one-site binding model (χ^2 = 4.8). Analysis with a two-site binding model with the assumption that the binding at each site generates the same change in CD signal improved the χ^2 value to 1.2. The equilibrium dissociation constants were determined to be 4.8 ± 1.4 and 120 ± 28 μM. Given the assumptions involved, these values are in reasonable agreement with values of 2.6 and 180 μM, respectively, previously determined (*20*) using the same technique but under slightly different buffer conditions. The corresponding titration with Mg^{2+} (Figure 2B) could be analyzed with a one-site binding model to give a dissociation constant (K_d) of 0.81 ± 0.12 mM, which is in agreement with the value of 0.7 mM estimated using competition with Ca^{2+} binding described in ref *20*.

Far-UV CD thermal unfolding studies are a useful method for screening for interaction partners because any ligand that binds to only the folded form of the protein will increase its stability toward thermal denaturation. The higher the affinity of the ligand, the greater the shift toward higher unfolding temperatures. We therefore performed thermal unfolding studies with F2 TnC in the presence and absence of Ca^{2+} and/or TnH peptides. Because the concentration of Mg^{2+} in muscle is in the millimolar range, we also probed the effects of this ion. The synthetic peptides used here, TnH(30−61) and TnH(126−159), correspond to the

Table 1: Transition Midpoint Temperatures (T_m) for Thermal Unfolding of F2 TnC (18 μM) in the Presence and Absence of Metal Ions and TnH Peptides

conditions	T_m (°C)
apo F2 TnC	40.6
35 μM TnH(30−61)	> 70[a]
35 μM TnH(126−159)	56.4
1 mM Ca^{2+}	74.6
1 mM Ca^{2+} and 35 μM TnH(30−61)	> 90
1 mM Ca^{2+} and 35 μM TnH(126−159)	79.0
1 mM Mg^{2+}	49.4
1 mM Mg^{2+} and 35 μM TnH(30−61)	> 85
1 mM Mg^{2+} and 35 μM TnH(126−159)	59.6

[a]F2 TnC complexes with peptides precipitate at > 70 °C in the absence of metal ions.

N-terminus and to a region containing the inhibitory and switch regions in vertebrates, respectively. F2 TnC in the absence of metal ions and peptides undergoes a single transition, presumably caused by unfolding of the C lobe, with a transition midpoint temperature (T_m) of 40.6 °C. When temperature unfolding was repeated in the presence of cations and/or peptides, the results (Table 1) suggest that Ca^{2+} binds significantly more strongly than Mg^{2+}, that the TnH peptides bind to both apo and metal-loaded forms of F2 TnC, and that TnH(30−61) binds more strongly than TnH(126−159).

Competition Studies of the Interaction of F2 TnC with TnH Peptides by Fluorescence. As in a previous study of the interaction of F1 TnC with the TnI peptides (*26*), we quantified the interactions by exploiting the fact that F2 TnC also binds with high affinity to melittin, a 26-residue peptide containing a single tryptophan. Binding of melittin was studied by monitoring the changes in tryptophan fluorescence associated with binding to F2 TnC, which contains no tryptophans (Figure 3A). The equilibrium dissociation constants for binding of melittin to F2 TnC are 20−25-fold weaker than those for F1 TnC, which have been remeasured in this study (Table 2). Equilibrium K_d values for the binding of the TnH(30−61) and TnH(126−159) peptides were determined using competition with melittin binding as previously described (*26*) (Figure 3B). The K_d values for the binding of TnH(30−61) to apo and holo F2 TnC [37.7 and 7.8 nM, respectively (see Table 2)] are some 10-fold higher than the corresponding values for F1 TnC. Interestingly, however, in this case, we observe that the effect of Ca^{2+} in increasing the strength of the interaction is significantly greater than for F1 TnC. The TnH(126−159) peptide binds much more weakly than does the TnH(30−61) peptide (Table 2). In this case, however, the affinities for F2 TnC and F1 TnC are very similar, as are the effects of Ca^{2+}.

Values measured in the presence of 5 mM Mg^{2+} are very similar to those measured with the apoproteins for both melittin and the TnH peptides. Values measured in the presence of 5 mM Mg^{2+} and 1 mM Ca^{2+} are essentially the same as those measured in the presence of 1 mM Ca^{2+}.

Ca^{2+} Binding Studies with Chromophoric Ca^{2+} Chelators. Initial experiments involving titration of a mixture of the chelator 5,5′-dibromo BAPTA [$K_{Ca} = (6.3 \pm 0.5) \times 10^5$ M^{-1}] and apo F2 TnC (1:1.5 ratio) with a stock solution of Ca^{2+} demonstrated that F2 TnC competed poorly with this high-affinity chelator. We therefore performed all further experiments with a lower-affinity chelator, 5-nitro BAPTA [with a K_{Ca} of $(4.1 \pm 0.3) \times 10^4$ M^{-1}]. Solutions of 5-nitro BAPTA (22 μM) and

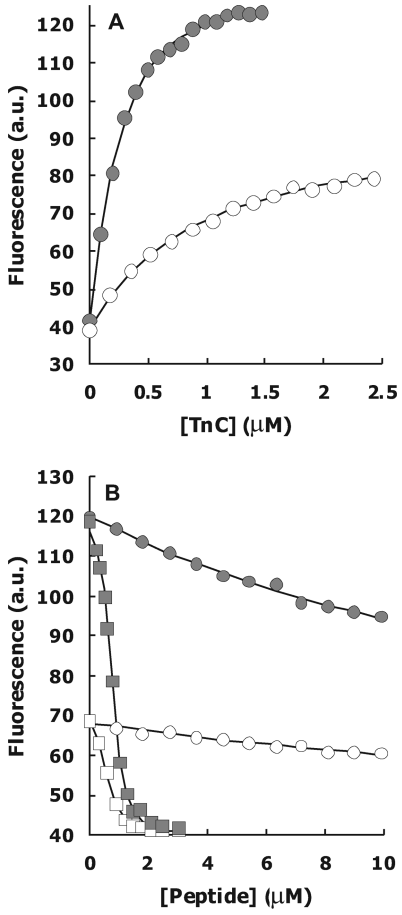

FIGURE 3: Competition experiments to determine the affinities of TnH peptides for F2 TnC. (A) Titration of melittin (0.33 μM) with F2 TnC in the presence (filled symbols) and absence (empty symbols) of 1 mM Ca^{2+}. (B) Titrations of melittin (0.33 μM) and F2 TnC with TnH(30−61) (squares) and TnH(126−159) (circles). F2 TnC concentrations were 1.4 and 2.4 μM for experiments performed in the presence (filled symbols) and absence (empty symbols) of 1 mM Ca^{2+}, respectively.

apo F2 TnC (32 μM) were titrated with Ca^{2+} in the presence and absence of the TnH peptides (65 μM), and the absorbance was measured at 430 nm (Figure 4). Stoichiometric Ca^{2+} dissociation constants were determined by direct fits to the experimental data as described in ref *31*. The results are summarized in Table 3. Titrations performed in the presence of Mg^{2+} demonstrate that this metal does not compete effectively with Ca^{2+} binding, although there is some evidence for weak competition at one site (K_d1 increases from 6.3 to 9.3 μM). In the case of the TnH peptides, there is clear evidence that Ca^{2+} binding is enhanced in the presence of the peptides. This is the expected result because we have shown that the peptides bind more strongly in the presence of Ca^{2+}.

TnH Peptide Binding Involves Both Lobes of F2 TnC. We then mapped the sites of interaction of the two peptides on F2 TnC by NMR spectroscopy. The NMR $^1H-^{15}N$ HSQC spectra of apo and holo F2 TnC have an excellent spectral dispersion indicating that both domains are intrinsically structured even in the absence of Ca^{2+}, in agreement with the CD data. This is at variance with what is observed for the C lobe of skeletal muscle TnC, which has in the apo form a spectrum with low chemical shift dispersion typical of random coils (*29*). Comparison of the HSQC spectra of the apo and holo forms of F2 TnC shows conclusively binding of two Ca^{2+} ions based on the

Table 2: Equilibrium Dissociation Constants for the Binding of Melittin and the TnH Peptides to F1 TnC and F2 TnC in the Presence and Absence of Metal Ions

peptide	metal[a]	K_d (F1 TnC)[b]	K_d (F2 TnC)	K_d (F2 TnC)/K_d (F1 TnC)
melittin	none	41 ± 9 nM (26 ± 7 nM)	0.84 ± 0.18 μM	20.5 ± 6.3
	Ca^{2+}	8.3 ± 2.1 nM (5.2 ± 1.2 nM)	0.19 ± 0.03 μM	22.9 ± 6.8
	Mg^{2+}	32 ± 6 nM	0.77 ± 0.12 μM	24.0 ± 5.8
TnH(30−61)	none	1.9 ± 0.6 nM (1.5 ± 0.5 nM)	37.7 ± 4.5 nM	19.8 ± 3.1
	Ca^{2+}	0.9 ± 0.2 nM (1.3 ± 0.3 nM)	7.8 ± 0.15 nM	8.7 ± 2.5
	Mg^{2+}	2.2 ± 0.4 nM	38.5 ± 5.2 nM	17.5 ± 3.3
	Ca^{2+} and Mg^{2+}	1.3 ± 0.4 nM	6.7 ± 0.9 nM	5.2 ± 1.2
TnH(126−159)	none	12.2 ± 3.4 μM (8.5 ± 3.7 μM)	15.5 ± 4.5 μM	1.3 ± 0.5
	Ca^{2+}	3.7 ± 1.1 μM (5.4 ± 1.5 μM)	3.1 ± 0.8 μM	0.85 ± 0.35
	Mg^{2+}	9.1 ± 3.2 μM	13.5 ± 3.5 μM	1.5 ± 0.6
	Ca^{2+} and Mg^{2+}	not determined	3.5 ± 0.8 μM	not determined

[a]Experiments were performed in the presence of 0.2 mM EGTA and 1 mM Ca^{2+} or 5 mM Mg^{2+}. [b]Data in parentheses are from ref *26*.

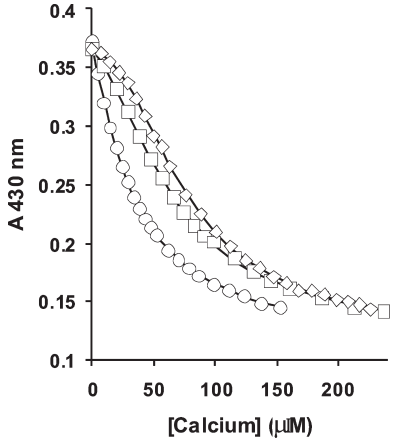

FIGURE 4: Titrations of 5-nitro BAPTA with Ca^{2+}. Spectrum of 5-nitro BAPTA (22 μM) alone (○), with 31.5 μM apo F2 TnC (□), or with 31.5 μM apo F2 TnC and 65 μM TnH(30−61) (◇).

Table 3: Stoichiometric Dissociation Constants for the Binding of Ca^{2+} to F2 TnC Measured in the Presence and Absence of Mg^{2+} and the TnH Peptides

sample	K_d1 (μM)	K_d2 (μM)	K_d1K_d2 (μM^2)
F2 TnC	6.3 ± 1.1	93 ± 15	580 ± 140
F2 TnC and 1 mM Mg^{2+}	9.3 ± 1.4	83 ± 11	780 ± 160
TnH(30−61)	2.4 ± 0.3	45 ± 8	110 ± 20
TnH(126−159)	3.7 ± 0.5	59 ± 12	220 ± 50

^{15}N chemical shift of the amide nitrogen of the residue in position 8 of a canonical EF-hand loop. The value of this observable is highly diagnostic of the presence of Ca^{2+} binding and provides a direct identification of the residues involved (*32*). The two other coordination sites are inactive even at high (millimolar) Ca^{2+}:protein molar ratios.

We titrated labeled Ca^{2+}-loaded F2 TnC with both TnH(30−61) (Figure 5A) and TnH(126−159) (Figure 5B) to reach saturation. In both cases, the spectra show progressive chemical shifts during the titration that are typical of a fast exchange regime on the NMR time scale. Similar resonances are affected by the two peptides, but overall, TnH(30−61) produces a stronger chemical shift perturbation at comparable peptide:protein molar ratios. To identify more specifically which lobe of F2 TnC is involved in the interaction without achieving full assignment of the spectrum of F2 TnC, we engineered two constructs spanning the sequence of each of the two lobes: NTnC (residues 1−88) and CTnC (residues 89−158). The NMR spectra of the two fragments are almost completely additive, and their superposition reproduces the spectrum of the full-length protein (Figure 5C). This additivity is observed for most of the individual domains of calmodulin-like proteins and tells us that the two lobes are independently folded and do not significantly influence each other structurally. Comparison of the spectra at the final points of the titrations (each titration was stopped when no further change was observed upon further addition of peptide) with those of the individual domains indicates that the interaction involves resonances of both lobes (Figures 5B,C), implying an overall structural rearrangement of F2 TnC upon TnH binding. This is at strong variance with what is observed for the same peptides with F1 TnC where interaction seems to involve only the C lobe (*26*) but is in good agreement with the behavior of vertebrate TnCs (*33*).

The TnH Peptides Compete for the Same Binding Site on F2 TnC. To test whether the two peptides compete for the same site and to detect any potential extra sites of interaction, we first saturated F2 TnC with the high-affinity TnH(30−61) peptide and then titrated this complex with the low-affinity TnH(126−159) peptide. The spectrum recorded at a 1:1 TnH(126−159):F2 TnC molar ratio is mostly superposable with that recorded in the absence of TnH(126−159) (Figure 6A), suggesting that, once TnH(30−61) is bound, the second peptide is not able to occupy additional binding sites. In contrast, when F2 TnC was first saturated with the low-affinity TnH(126−159) peptide and this complex was then titrated with TnH(30−61), most of the features observed in the presence of just TnH(30−61) reappeared (Figure 6B). These results support the hypothesis that the two peptides compete for the same site.

DISCUSSION

We have characterized here the structural features of the F2 isoform of *Lethocerus* TnC and the properties of its binding to TnH. We have also explored how the affinities of TnC for TnH are affected by the presence of Ca^{2+} and/or Mg^{2+}. It is interesting to compare our findings with what is known for vertebrate TnCs and for the *Lethocerus* isoform F1 TnC, responsible for stretch activation (*20*). Structurally, F2 TnC seems to share most of the properties already described for F1 TnC (*26*, *34*): both lobes are structured and are mainly helical also in the absence of Ca^{2+}, a property at variance with that of the C lobe of skeletal TnC in which this domain is completely unstructured in the absence of Ca^{2+} (*29*). Interaction with TnH was tested using two peptides

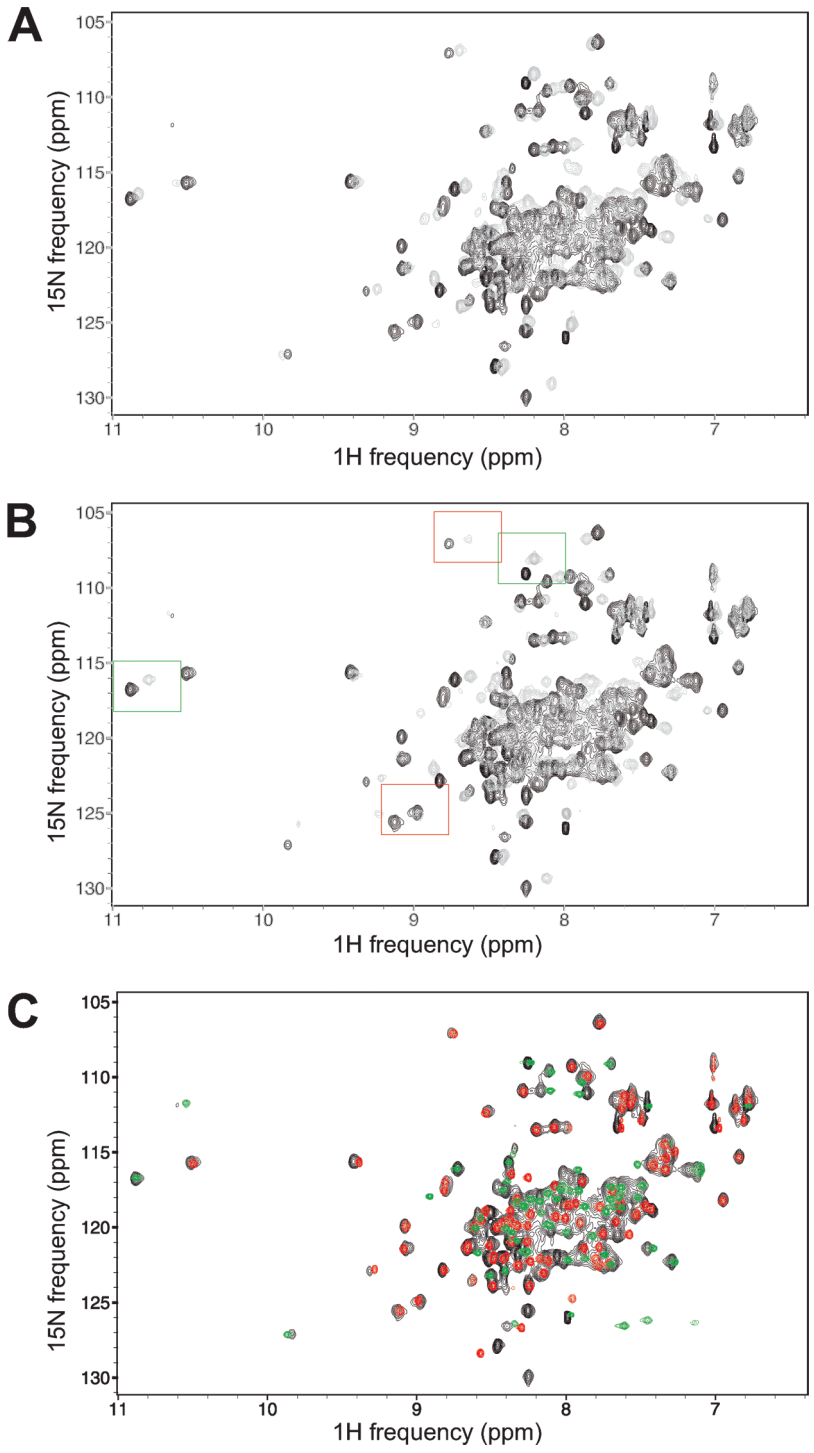

FIGURE 5: Titration of F2 TnC with TnH peptides as followed by NMR spectroscopy and mapping of the interactions onto the individual lobes. (A) Superposition of the HSQC spectrum of Ca^{2+}-loaded F2 TnC (black) with the final point of a titration with TnH(126−159) (gray) (1:2.5 molar ratio). (B) Same as panel A but for the TnH(30−61) peptide (1:1.3 molar ratio). Red and green boxes are examples of resonances from the N and C lobes, respectively, which can be judged by comparing the spectra in panel C. (C) Comparison of the spectra of full-length F2 TnC (black) and of the N- and C-terminal lobes (red and green, respectively). All spectra were recorded at 600 MHz and 25 °C.

spanning the N-terminus and the region of TnH that corresponds to the inhibitory and switch peptide in vertebrate muscle (*35*). These are the regions that anchor TnI and activate contraction in vertebrate muscles (see ref *5* and references cited therein); the same peptides were also found to interact with F1 TnC (*26*). We obtain a K_d in the nanomolar range for binding of F2 TnC to TnH(30−61) that reveals a somewhat tighter interaction compared to that observed for vertebrate skeletal TnC, i.e., 8 nM compared to 48 nM in the presence of Ca^{2+} (*28*). The corresponding value for binding of TnH(126−159) to F2 TnC is in the micromolar range and again approximately comparable to that of vertebrate TnC.

An even more important comparison of our findings with the K_d values observed for F1 TnC using the same peptides (*26*) should be conducted. The interaction of F2 TnC with TnH has several important different features compared to that of the F1 TnC isoform. First, the interaction is modulated by Ca^{2+}, while F1 TnC seems to be entirely insensitive to Ca^{2+} (*26*). We could

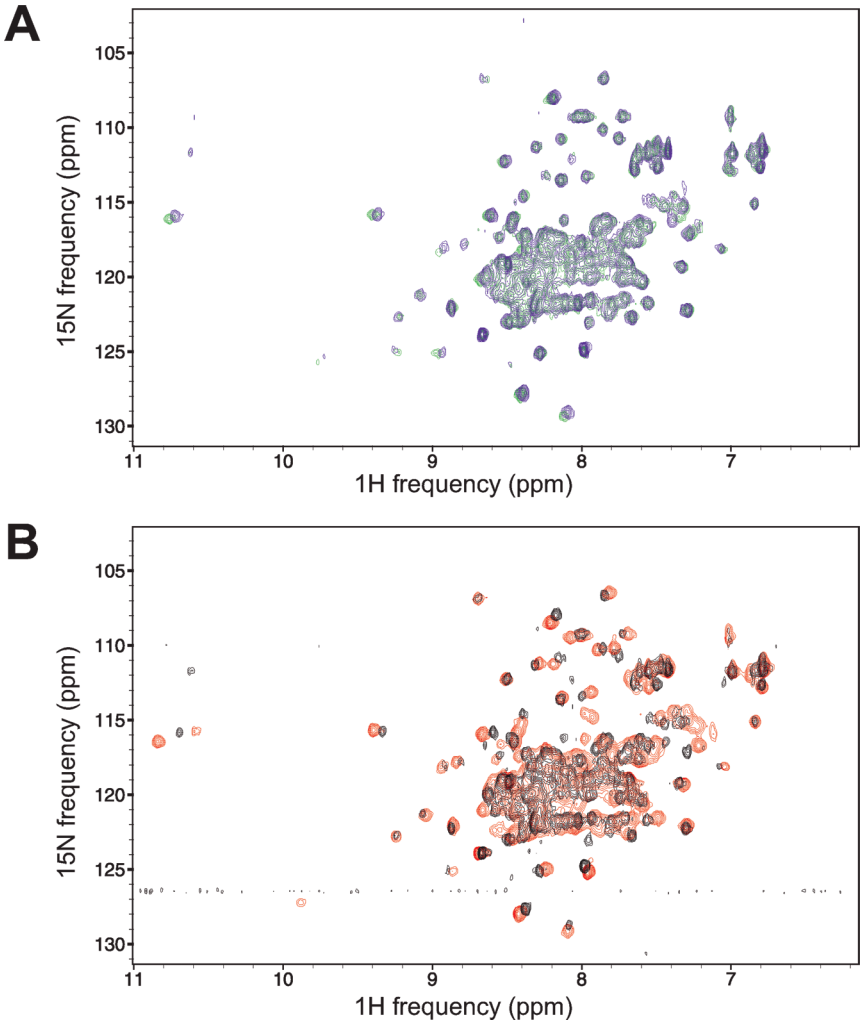

FIGURE 6: Testing whether the peptides compete for the same site of F2 TnC. (A) Superposition of the HSQC spectra recorded at the final points of the titrations of F2 TnC with TnH(30−61) (green) and with both TnH(30−61) and TnH(126−159) (blue). (B) Superposition of the HSQC spectra recorded at the final points of the titrations of F2 TnC with TnH(126−159) (red) and with both TnH(126−159) and TnH(30−61) (black). All spectra were recorded at 600 MHz and 25 °C.

confirm this observation using three independent approaches that go from probing the effect of Ca^{2+} on the melting points of F2 TnC in the absence and in presence of the peptides to a quantification of the dissociation constants by competition experiments. A Ca^{2+} dependence of the interaction for F2 TnC but not for F1 TnC can be explained by the presence of an extra Ca^{2+} binding site in the regulatory N lobe of F2 TnC that is absent in F1 TnC. The current evidence suggests that the calcium concentration in *Lethocerus* should not be sufficiently high to allow full occupancy of the two sites (*20*, *21*). We also probed the interactions in the presence of an excess of Mg^{2+} to mimic the muscle ion concentrations. Although Mg^{2+} is constantly present at high concentrations in muscles and is therefore an important component that is customarily used in mechanical measurements, most of the in vitro assays aiming at quantifying the binding affinities of TnI fragments have been conducted in the absence of this cation. This choice was probably dictated by the reasonable assumption that, because Mg^{2+} does not alter dramatically the structure of TnC (*36*), it should not be of primary importance. Interestingly, we observe for both F1 and F2 TnCs that the presence of Mg^{2+} does modulate the affinities but does not substantially alter their ratios.

The second noticeable difference from F1 TnC is that for this isoform the peptide−TnC interaction involves only the C lobe, leaving the N lobe idle (*26*). This behavior is very different from what we observed here for F2 TnC where the peptides have profound effects on the whole spectrum and affect resonances of residues from both the N lobe and the C lobe, indicating that the mode of binding of the two isoforms to the same TnH peptides is very different.

Finally, whether in an ion-loaded or ion-free form, F2 TnC has overall lower affinities for TnH(30−61) compared to those of F1 TnC by approximately 1 order of magnitude, whereas the affinities for TnH(126−159) are comparable. This seems to be at variance with recent estimates by isothermal titration calorimetry of the K_d values of F1 and F2 TnCs with a long N-terminal TnH fragment [TnH(1−224)] that contains both peptides and with the observation that, upon replacement of F1 and F2 TnC in different proportions to reproduce the behavior of native fibers, the maximal work is produced at excess F1:F2 molar ratios (i.e., 50−100:1) (*24*). While accurate quantification of the interactions at the level of the longer TnH construct might be biased by the strong tendency of the protein to aggregate, the relative differences in K_d values observed for the longer TnH(1−224) (1 μM for F1 TnC and 23 nM for F2 TnC) could well reflect the presence of additional interactions formed by F2 TnC with regions of TnH outside the peptides tested here and/or conformational effects that can be observed only at the level of long TnH constructs.

Taken together, our results all suggest a much greater similarity of F2 TnC to the vertebrate muscle orthologs than to F1 TnC. In agreement with this hypothesis is the observation that TnH(1−224) has an affinity for F2 TnC closer to that of cardiac TnI for TnC [i.e., ~8 nM (*24*, *37*)]. We therefore propose that the structure and the main mechanism of action of F2-mediated contraction are also more similar to those of vertebrate muscle, whereas we expect that the F1 TnC−TnH−TnT complex will be significantly different.

What do these observations tell us about the mechanism operating in insect flight muscles responsible for stretch activation?

The role of binding of Ca^{2+} to F2 TnC seems to be, as in vertebrate muscle, twofold. On one hand, it confers specific properties that facilitate the anchoring of the C lobe to the N-terminus of TnI and/or TnH. Especially tight affinities of F1 TnC could well be required because of the need for greater resistance to forces arising from the greater stiffness of flight muscle fibers (*17*). On the other hand, we expect that the Ca^{2+} bound to the N lobe of F2 TnC but not of F1 TnC will act as the sensor that triggers and regulates the contraction during the preparatory phases of the flight. When the system has been sufficiently warmed up, the much more abundant F1 TnC isoform will come into action. The extent to which F2 TnC is activated by Ca^{2+} also affects the work done during oscillatory contraction by limiting the range of Ca^{2+} concentration over which the muscle performs maximal work (*24*). Recently, EM and X-ray diffraction studies on *Lethocerus* flight muscle have confirmed the presence of "troponin bridges" extending from troponin on the thin filament to myosin on the thick filament (*38*, *39*). It was proposed that during stretch activation, troponin bridges pull on tropomyosin to expose myosin binding sites on actin, according to the steric blocking model (*39*). If troponin bridges contain the extended C-terminal tail of TnH (*24*, *40*), stretch may act through the troponin complex to displace tropomyosin on actin as long as Ca^{2+} is bound to F1 TnC. Alternatively, the N lobe of F1 TnC may interact with an as yet unidentified partner extending from the thick filament in a troponin bridge. In this case, mechanical stress on F1 TnC might have the same effect as Ca^{2+} binding to the N lobe of F2 TnC.

While much work is still needed to clarify the exact mechanism of stretch activation, this paper contributes to our comprehension of the phenomenon and provides clear suggestions about where to direct our future efforts. We expect that a real breakthrough may come only when the structure of the F1 troponin complex becomes available.

ACKNOWLEDGMENT

We thank Steve Howell for mass spectrometry analysis.

REFERENCES

1. Hooper, S. L., Hobbs, K. H., and Thuma, J. B. (2008) Invertebrate muscles: Thin and thick filament structure; molecular basis of contraction and its regulation, catch and asynchronous muscle. *Prog. Neurobiol. 86*, 72–127.
2. Li, M. X., Wang, X., and Sykes, B. D. (2004) Structural based insights into the role of troponin in cardiac muscle pathophysiol. *J. Muscle Res. Cell Motil. 25*, 559–579.
3. Gordon, A. M., Homsher, E., and Regnier, M. (2000) Regulation of contraction in striated muscle. *Physiol. Rev. 80*, 853.
4. Vibert, P., Craig, R., and Lehman, W. H. (1997) Steric-model for activation of muscle thin filaments. *J. Mol. Biol. 266*, 8–14.
5. Hoffman, R. M., and Sykes, B. D. (2007) Disposition and dynamics: Interdomain orientations in troponin. *Adv. Exp. Med. Biol. 592*, 59–70.
6. Greaser, M. L., and Gergely, J. (1971) Reconstitution of troponin activity from three protein components. *J. Biol. Chem. 246*, 4226–4233.
7. Herzberg, O., and James, M. N. G. (1985) Structure of the calcium regulatory muscle protein troponin C at 28 Å resolution. *Nature 313*, 653–659.
8. Herzberg, O., and James, M. N. G. (1988) Refined crystal structure of troponin C from turkey skeletal muscle at 2.0 Å resolution. *J. Mol. Biol. 203*, 761–779.
9. Satyshur, K. A., Rao, S. T., Pyzalska, D., Drendel, W., Greaser, M., and Sundaralingam, M. (1988) Refined structure of chicken skeletal muscle troponin C in the two-calcium state at 2-Å resolution. *J. Biol. Chem. 263*, 1628–1647.
10. Slupsky, C. M., and Sykes, B. D. (1995) NMR solution structure of calcium saturated skeletal muscle troponin C. *Biochemistry 34*, 15953–15964.
11. Houdusse, A., Love, M. L., Dominguez, R., Grabarek, Z., and Cohen, C. (1997) Structures of four Ca^{2+}-bound troponin C at 2.0 Å resolution: Further insights into the Ca^{2+}-switch in the calmodulin superfamily. *Structure 5*, 1695–1711.
12. Vassylyev, D. G., Takeda, S., Wakatsuki, S., Maeda, K., and Maeda, Y. (1998) Crystal structure of troponin C in complex with troponin I fragment at 2.3-Å resolution. *Proc. Natl. Acad. Sci. U.S.A. 95*, 4847–4852.
13. Mercier, P., Spyracopoulos, L., and Sykes, B. D. (2001) Structure, Dynamics, and Thermodynamics of the Structural Domain of Troponin C in Complex with the Regulatory Peptide 1−40 of Troponin I. *Biochemistry 40*, 10063–10077.
14. Takeda, S., Yamashita, A., Maeda, K., and Maeda, Y. (2003) Structure of the core domain of human cardiac troponin in the Ca^{2+}-saturated form. *Nature 424*, 35–41.
15. Vinogradova, M. V., Stone, D. B., Malanina, G. G., Kartzaferi, C., Cooke, R., Mendelson, R. A., and Fletterick, R. J. (2005) Ca^{2+}-regulated structural changes in troponin. *Proc. Natl. Acad. Sci. U.S.A. 102*, 5038–5043.
16. Pringle, J. M. (1949) The excitation and contraction of the flight muscle of insects. *J. Physiol. 108*, 226–232.
17. Pringle, J. W. (1978) The Croonian Lecture, 1977. Stretch activation of muscle: Function and mechanism. *Proc. R. Soc. London, Ser. B 201*, 107–130.
18. Thorson, J., and White, D. C. (1983) Role of cross-bridge distorsion in the small-signal mechanical dynamics of insect and rabbit striated muscle. *J. Physiol. 343*, 59–64.
19. Josephson, R. K., Malamud, J. G., and Stokes, D. R. (2000) Asynchronous muscle: A primer. *J. Exp. Biol. 203*, 2713–2722.
20. Agianian, B., Kržič, U., Qiu, F., Linke, W. A., Leonard, K., and Bullard, B. (2004) A troponin switch that regulates muscle contraction by stretch instead of calcium. *EMBO J. 23*, 772–779.
21. Linari, M., Reedy, M. K., Reedy, M. C., Lombardi, V., and Piazzesi, G. (2004) Ca-activation and stretch-activation in insect flight muscle. *Biophys. J. 87*, 1101–1111.
22. Gordon, S., and Dickinson, M. H. (2006) Role of calcium in the regulation of mechanical power in insect flight. *Proc. Natl. Acad. Sci. U.S.A. 103*, 4311–4315.
23. Qiu, F., Lakey, A., Agianian, B., Hutchings, A., Butcher, G. W., Labeit, S., Leonard, K., and Bullard, B. (2003) Troponin C in different insect muscle types: Identification of two isoforms in *Lethocerus*, *Drosophila* and *Anopheles* that are specific to asynchronous flight muscle in the adult insect. *Biochem. J. 371*, 811–821.
24. Kržič, U., and Rybin, V.; et al. (2010) Regulation of oscillatory contraction in insect flight muscle by troponin. *J. Mol. Biol. 397*, 110–118.
25. Bullard, B., Leonard, K., Larkins, A., Butcher, G., Karlik, C., and Fyberg, E. (1988) Troponin of asynchronous flight muscle. *J. Mol. Biol. 204*, 621–637.
26. De Nicola, G., Burkart, C., Qiu, F., Agianian, B., Labeit, S., and Martin, S.; et al. (2007) The structure of *Lethocerus* troponin C: Insights into the mechanism of stretch activation in muscles. *Structure 15*, 813–824.
27. Tripet, B., van Eyk, J. E., and Hodges, R. S. (1997) Mapping of a second actin-tropomyosin and a second troponin C binding site within the C terminus of troponin I, and their importance in the Ca^{2+}-dependent regulation of muscle contraction. *J. Mol. Biol. 271*, 728–750.
28. Tripet, B., de Crescenzo, G., Grothe, S., O'Connor-McCourt, M., and Hodges, R. S. (2003) Kinetic analysis of the interactions between Troponin C (TnC) and Troponin I (TnI) binding peptides: Evidence for separate binding sites for the 'structural' N-terminus and the 'regulatory' C-terminus of TnI on TnC. *J. Mol. Recognit. 16*, 37–53.

29. Mercier, P., Li, M. K., and Sykes, B. D. (2000) Role of the structural domain of troponin C in muscle regulation: NMR studies of Ca^{2+} binding and subsequent interactions with regions 1−40 and 96−115 of troponin I. *Biochemistry 39*, 2902–2911.
30. Phan, J., Zdanov, A., Evdokimov, A. G., Tropea, J. E., Peters, H. P. K., Kapust, R. B., Li, M., Wlodawer, A., and Waugh, D. S. (2002) Structural basis for the substrate specificity of tobacco etch virus protease. *J. Biol. Chem. 277*, 50564–50572.
31. Linse, S. A., Helmersson, A., and Forsen, S. (1991) Calcium binding to calmodulin and its globular domains. *J. Biol. Chem. 266*, 8050–8054.
32. Biekofsky, R. R., Martin, S. R., Browne, J. P., Bayley, P. M., and Feeney, J. (1998) Ca^{2+} coordination to backbone carbonyl oxygen atoms in calmodulin and other EF-hand proteins. ^{15}N chemical shifts as probes for monitoring individual site Ca^{2+} coordination. *Biochemistry 37*, 7617–7629.
33. McKay, R. T., Tripet, B. P., Pearlstone, J. R., Smillie, L. B., and Sykes, B. D. (1999) Defining the Region of Troponin-I that Binds to Troponin-C. *Biochemistry 38*, 5478–5489.
34. De Nicola, G., Martin, S., Bullard, B., and Pastore, A. (2010) The solution structure of the apo C-terminal domain of *Lethocerus* F1 troponin C isoform. *Biochemistry 49*, 1719–1726.
35. Syska, H., Wilkinson, J. M., Grand, R. J. A., and Perry, S. V. (1976) The relationship between biological activity and primary structure of troponin I from white skeletal muscle of the rabbit. *Biochem. J. 153*, 375–387.
36. Finley, N. L., Howarth, J. W., and Rosevear, P. R. (2004) Structure of the Mg^{2+}-loaded C-lobe of cardiac troponin C bound to the N-domain of cardiac troponin I: Comparison with the Ca^{2+}-loaded structure. *Biochemistry 43*, 11371–11379.
37. Calvert, M. J., Ward, D. G., Trayer, H. R., and Trayer, I. P. (2000) The importance of the carboxyl-terminal domain of cardiac troponin C in Ca^{2+}-sensitive muscle regulation. *J. Biol. Chem. 275*, 32508–32515.
38. Wu, S., Liu, J., Reedy, M. C., Tregear, R. T., Winkler, H., Franzini-Armstrong, C., Sasaki, H., Lucaveche, C., Goldman, Y. E., Reedy, M. K., and Taylor, K. A. (2010) Electron tomography of cryofixed, isometrically contracting insect flight muscle reveals novel actin-myosin interactions. *PLoS One 5*, No. e12643.
39. Perz-Edwards, R. J., Irving, T. C., Baumann, B. A. J., Gore, D., Hutchinson, D. C., Kržič, U., Portera, R. L., Warde, A. B., and Reedy, M. K. (2011) X-ray diffraction evidence for myosin-troponin connections and tropomyosin movement during stretch activation of insect flight muscle. *Proc. Natl. Acad. Sci. U.S.A. 108*, 120–125.
40. Reedy, M. C., Reedy, M. K., Leonard, K. R., and Bullard, B. (1994) Gold/Fab immuno electron microscopy localisation of troponin H and troponin T in *Lethocerus* flight muscle. *J. Mol. Biol. 239*, 52–67.
41. Sreerama, N., and Woody, R. W. (2000) Estimation of protein secondary structure from circular dichroism spectra: Comparison of CONTIN, SELCON, and CDSSTR methods with an expanded reference set. *Anal. Biochem. 287*, 252–260.